Journal of Power Sources 195 (2010) 5481–5486

Contents lists available at ScienceDirect

Journal of Power Sources

journal homepage: www.elsevier.com/locate/jpowsour

Fracture process of nonstoichiometric oxide based solid oxide fuel cell under oxidizing/reducing gradient conditions

Kazuhisa Sato[a,b,*], Keiji Yashiro[a,b], Tatsuya Kawada[c], Hiroo Yugami[b], Toshiyuki Hashida[b,d], Junichiro Mizusaki[a,b]

[a] Institute of Multidisciplinary Research for Advanced Materials, Tohoku University, Japan
[b] Graduate School of Engineering, Tohoku University, Japan
[c] Graduate School of Environmental Studies, Tohoku University, Japan
[d] Fracture and Reliability Research Institute, Tohoku University, Japan

ARTICLE INFO

Article history:
Received 3 March 2010
Received in revised form 22 March 2010
Accepted 25 March 2010
Available online 1 April 2010

Keywords:
Solid oxide fuel cell (SOFC) laminate
Nonstoichiometry
Fracture process
Chemically induced stress
Finite element method (FEM)
Acoustic emission (AE) method

ABSTRACT

The influence of chemically induced expansion on the fracture damage of a nonstoichiometric oxide (ceria) based solid oxide fuel cell (SOFC) single cell laminate was investigated by using numerical stress analyses under oxidizing/reducing gradient condition. The single cell examined in this study was composed of electrolyte ($Ce_{0.8}Sm_{0.2}O_{2-\delta}$), anode (Cermets of Ni–$Ce_{0.8}Sm_{0.2}O_{2-\delta}$), and cathode ($La_{0.6}Sr_{0.4}Co_{0.2}Fe_{0.8}O_{3-\delta}$), respectively. The finite element method (FEM) was employed to calculate the residual stress, thermal stresses, and chemically induced expansion stresses for the single cell. The residual and thermal stresses were calculated much smaller than the fracture strength of the individual components of the single cell. On the other hand, the chemically induced expansion stresses were shown to remarkably increase for the temperature range greater than 973 K and accounted their magnitude for primary part of the induced stress. It was shown from the FEM that the maximum circumferential stress induced in the single cell exceeded the fracture strength of the individual components at the onset of the fracture damage detect by acoustic emission (AE) method.

1. Introduction

Solid oxide fuel cells (SOFC) can achieve an extremely high power generation efficiency, and thus are attracting attention as a next-generation fuel cell system [1]. High-performance SOFCs are currently being developed for practical use in various countries throughout the world [2,3].

Achieving practical SOFCs will require more than just improvement in power generation performance; ensuring reliability and durability will also be crucial. On the other hand, their main component material is mechanically brittle ceramic with low fracture toughness, and they may also contain materials which have the property of expanding or contracting in oxidizing/reducing conditions. Therefore, in the operating condition, there is a possibility of fracture due not only to thermal stress but also to chemically induced expansion or contraction [4–6,10]. For this reason, the mechanical and chemical properties of the component materials, and evaluation of the reliability of the SOFC in the operating condition are extremely important. In order to address the above issues, we have developed methods to enable comprehensive evaluation of interactions between mechanical and electrochemical factors, for characterization of component element materials and cell evaluation [7–9]. In particular, it is essential to develop and establish stress analysis and other SOFC design/evaluation techniques coupled with numerical analysis, to prevent a decline in SOFC performance due to problems such as mechanical damage. In this paper, the authors evaluated mechanical/chemical properties of the components for SOFC comprised of ceria based electrolyte, and conducted experiments and numerical calculations to evaluate the mechanical properties of the single cell under oxidizing/reducing gradient conditions. A stress analysis method taking chemically induced expansion into account was developed for single cell evaluation, and studies were conducted using this method to identify fracture conditions. The aim is to develop a foundation of SOFC design/evaluation methods which take into account mechanical and electrochemical factors.

* Corresponding author at: Institute of Multidisciplinary Research for Advanced Materials, Tohoku University, 2-1-1 Katahira, Aoba-ku, Sendai 980-8577, Japan. Tel.: +81 22 217 5341; fax: +81 22 217 5343.
E-mail address: kazuhisa@tagen.tohoku.ac.jp (K. Sato).

0378-7753/$ – see front matter © 2010 Elsevier B.V. All rights reserved.
doi:10.1016/j.jpowsour.2010.03.077

2. Experimental and calculation

2.1. Evaluation of mechanical/chemical properties of component materials

The single cell examined in this study was composed of ($Ce_{0.8}Sm_{0.2}O_{2-\delta}$) electrolyte material, Ni–$Ce_{0.8}Sm_{0.2}O_{2-\delta}$ (60:40 wt%) anode material, and $La_{0.6}Sr_{0.4}Co_{0.2}Fe_{0.8}O_{3-\delta}$ cathode material. The small punch (SP) test method was used to evaluate the mechanical properties of each component material [7]. The elastic modulus at 873 K under an inert gas (argon) condition was determined by small punch (SP) testing method using miniaturized disk specimens. The load application was performed using a puncher, at a crosshead speed of 0.1 mm min^{-1} until final failure occurred. The deflections of the specimens were measured by monitoring the movement of an Al_2O_3 rod using a linear variable differential transducer (LVDT) attached to the testing apparatus. The load application was conducted using a screwdriver type testing apparatus. A molybdenum heating element was used to conduct the high-temperature SP tests. Prior to the SP tests, the chamber was evacuated up to 10^{-1} Pa, and then argon gas was introduced into it. The test temperature was 873 K. The specimens were heated to the test temperature at a rate of 100 K h^{-1} and allowed to stand for a minimum of 2 h before proceeding with the measurement. The deformation and stress analyses for the SP tests were performed using a finite element method (FEM) assuming a linear elastic response. In this study, numerical data were used to compute the elastic modulus. The elastic modulus of the SP specimens can be expressed by the following equation [7]:

$$E_{SP} = f(t/a)\frac{3a^2P(1-\nu)(3+\nu)}{4\delta\pi t^3}$$

where P denotes the load; δ, the deflection at the specimen center; ν, Poisson's ratio; t, the specimen thickness (=0.7 mm); a, the bore diameter of the lower die (=2.38 mm); and $f(t/a)$, the correction factor for the specimen thickness (=1.13). The value of ν was assumed to be 0.33 in accordance with the reported data for doped ceria ceramics [11].

A differential dilatometer modified to enable control of the oxygen partial pressure condition was used to measure the amount of chemically induced expansion of the $Ce_{0.8}Sm_{0.2}O_{2-\delta}$ used in the electrolyte and anode materials. The amount of contraction was measured by varying the oxygen partial pressure while maintaining a fixed testing temperature. The amount of chemically induced expansion was determined by using Al_2O_3, which does not experience chemically induced expansion, as a reference specimen, and detecting the difference in the amount of expansion with $Ce_{0.8}Sm_{0.2}O_{2-\delta}$ while varying the measurement atmosphere. The test specimen was shaped as a flat plate (dimensions: 2.3 mm × 0.5 mm × 15 mm). Testing temperatures were 873 K, 973 K and 1073 K. A blended gas of H_2/Ar/H_2O was used as the atmospheric gas, and the atmosphere was varied in steps from an oxidizing condition to a reducing condition (approximately 10^{-18} atm). Oxygen partial pressure in the specimen chamber was measured using a zirconia oxygen sensor. Immediately after varying the oxygen partial pressure, a transitional phenomenon was seen in the chemically induced expansion behavior of $Ce_{0.8}Sm_{0.2}O_{2-\delta}$. It was observed that, as the oxygen partial pressure increases or decreases, the length increases or decreases over time, but over a period of a few minutes, it reaches a fixed amount of expansion or contraction. Under all conditions, conditions were maintained until the amount of expansion or contraction levelled off, and the relationship between the amount of chemically induced expansion and the oxygen partial pressure was determined based on the values measured in the steady state.

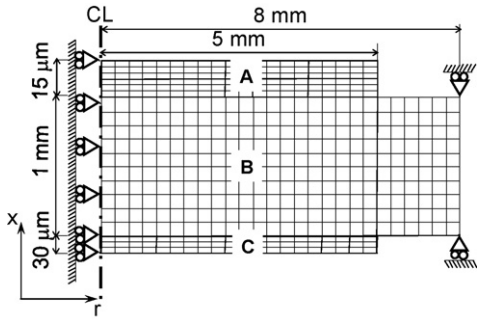

Fig. 1. FEM model of the single cell used. A: cathode, B: electrolyte, and C: anode.

2.2. Calculation

This section describes the finite element method (FEM) conducted for the fracture experiment on a single cell. Fracture conditions were examined by using the results of evaluating mechanical/chemical properties described above, and conducting stress analysis of a fracture experiment [7] conducted by the authors using a flat disc single cell. ABAQUS was used as the analysis code. Fig. 1 shows the element breakdown of the analyzed single cell with flat disc shape. It is a laminated disc formed from three layers—an anode, electrolyte and cathode—and the dimensions of each are the same as in experiment [7]. The axial symmetric model shown in Fig. 1 was used to take into account symmetry about the central axis of the single cell. This calculation takes into account residual stress produced at the time of single cell fabrication, thermal stress, and stress due to chemically induced expansion of $Ce_{0.8}Sm_{0.2}O_{2-\delta}$. Residual stress is the stress produced when the temperature drops from the 1300 K sintering temperature of the single cell to 298 K. Thermal stress is the stress which occurs when the temperature rises from 298 K to the specified temperature (873 K, 973 K, 1073 K). Only steady state analysis was conducted due to the fact that the heating speed used in the experiment was sufficiently slow, and thickness of the test specimen single cell was small. That is, thermal stress analysis was conducted assuming that temperature inside the single cell is fixed. Stress also arises due to chemically induced expansion of the electrolyte material and anode material used in this research. Stress arising due to chemically induced expansion can be analyzed using the same method as for thermal stress analysis. That is, the method evaluates strain due to chemically induced expansion corresponding to the oxygen partial pressure (oxygen potential) of each position at the specified temperature, and the stress is estimated by calculating the internal strain. In the single cell fracture experiment described above, the oxygen partial pressure distribution occurring inside the cell was found analytically using the method indicated in Appendix A. Table 1 gives the thermal expansion coefficients for the component materials used in the calculation. However, no value is given in the literature for the anode material in this research, and thus it was estimated using the rule of mixtures based on the literature values for $Ce_{0.8}Sm_{0.2}O_{2-\delta}$ and Ni. Strain of the anode material due to chemically induced expansion was also estimated based on the rule of mixtures. However, there is assumed to be no chemically induced expansion of Ni. It is known from the results of numerical

Table 1
Thermal expansion of the single cell components used.

Component	Thermal expansion (×10^{-6} K^{-1})
Electrolyte	11.2
Anode	12.0
Cathode	12.5 [10]

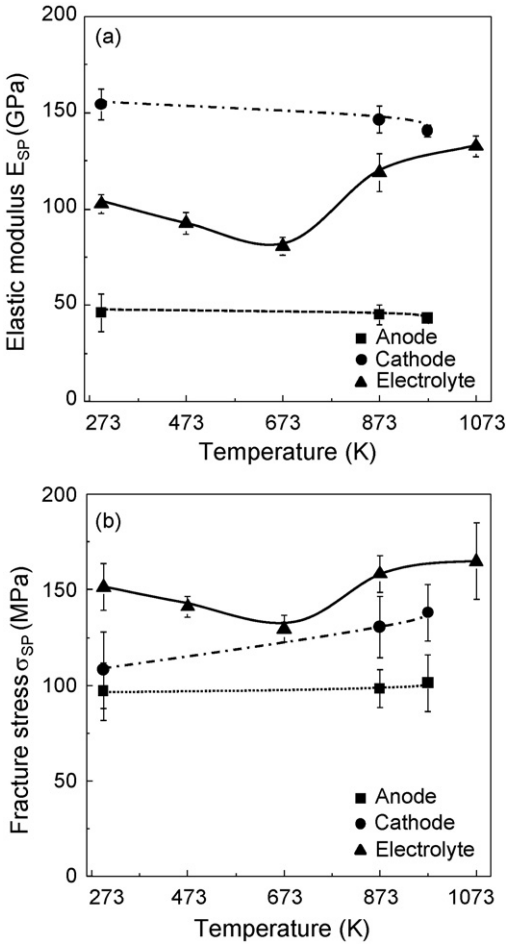

Fig. 2. Mechanical properties of anode (Cermets of Ni-20SDC), electrolyte ($Ce_{0.8}Sm_{0.2}O_{2-\delta}$), and cathode ($La_{0.6}Sr_{0.4}Co_{0.2}Fe_{0.8}O_{3-\delta}$) as a function of testing temperature determined by SP method. (a) Elastic modulus (E_{SP}) and (b) fracture stress (σ_{fSP}).

calculation that the effects of chemically induced expansion of the anode can be ignored.

3. Results and discussion

3.1. Mechanical and chemical properties of component materials

Mechanical properties of the component materials were evaluated using the SP testing method, in order to examine fracture conditions based on stress analysis of the single cell. Fig. 2 shows temperature dependence of the elastic modulus and fracture strength of the anode, electrolyte and cathode materials, obtained through SP testing. This experiment showed that all component materials exhibit brittle fractures.

For the electrolyte material, the elastic modulus and fracture strength decrease as temperature rises from room temperature to 400 K, and both show a tendency to increase in response to further temperature rises. On the other hand, the elastic modulus of the cathode material and anode material tends to drop somewhat as the temperature increases. Fracture strength, in contrast, tends to increase monotonically with temperature. The mechanisms underlying the temperature dependence of mechanical properties are unknown at the present stage. However, for the electrolyte material, unusual variation behavior is exhibited near 500 K, where the oxygen nonstoichiometry of the material begins to appear, and thus it is conjectured that the mechanical properties of the electrolyte

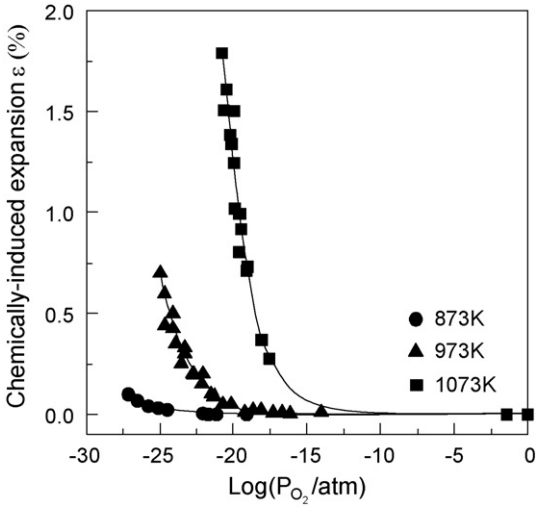

Fig. 3. Chemically induced expansion of $Ce_{0.8}Sm_{0.2}O_{2-\delta}$ as a function of oxygen partial pressure.

material may vary due to changes in oxygen partial pressure. In the future, it will be necessary to examine the effects of factors such as oxygen partial pressure on mechanical properties.

Next, Fig. 3 shows the relationship between the amount of chemically induced expansion and oxygen partial pressure for $Ce_{0.8}Sm_{0.2}O_{2-\delta}$. The length variations were thus measure range of 873–1073 K. In this figure, the specimen length in the stoichiometric state ($\delta = 0$) at each temperature chosen as a reference, and the deviations from the reference (ΔL) are normalized to the full length at room temperature (L_0) to be plotted against $\log(P_{O_2}/\text{atm})$. The most of the measured length variations were in good reversibility. It was found that chemically induced expansion occurs under an oxygen partial pressure environment of about 10^{-18} atm at 873 K, about 10^{-15} atm at 973 K and about 10^{-12} atm at 1073 K. Atkinson [4,11] reports this phenomenon in connection with the oxygen nonstoichiometry of $Ce_{0.8}Gd_{0.2}O_{2-\delta}$. In this research too, let us examine the relationship with chemically induced expansion, based on data on the amount of oxygen nonstoichiometry of $Ce_{0.8}Sm_{0.2}O_{2-\delta}$ reported by Kobayashi et al. [12]. As shown in Fig. 4, there is an almost linear relationship between the amount of oxygen nonstoichiometry and the amount of chemically induced expansion for $Ce_{0.8}Sm_{0.2}O_{2-\delta}$. Therefore, if the least-squares method is applied to the results in Fig. 4 for

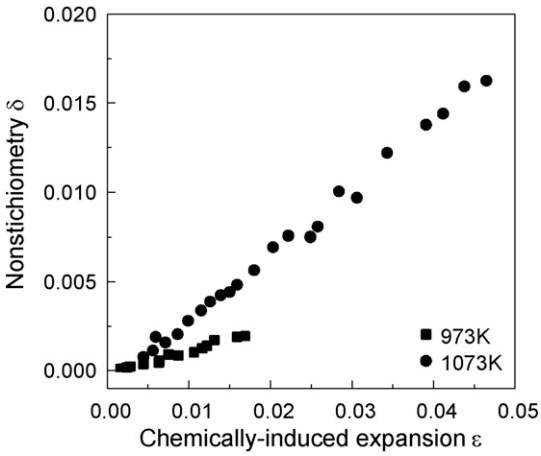

Fig. 4. Relationship between the nonstoichiometry [12] and chemically induced expansion for $Ce_{0.8}Sm_{0.2}O_{2-\delta}$.

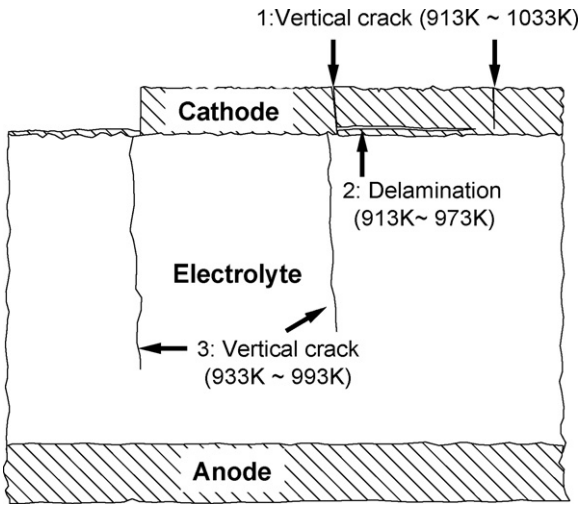

Fig. 5. Schematic of fracture pattern of $Ce_{0.8}Sm_{0.2}O_{2-\delta}$ based SOFC single cell.

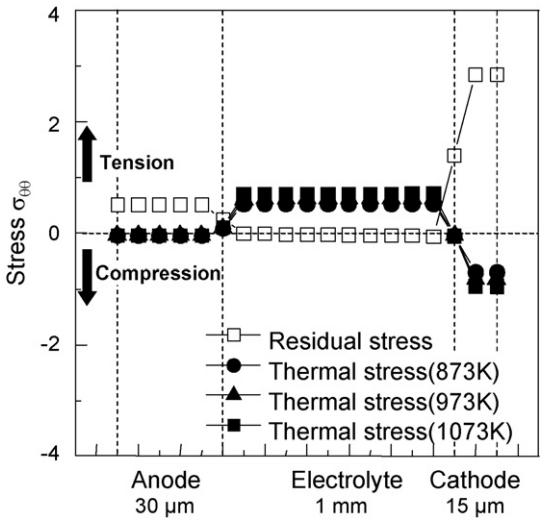

Fig. 6. Residual stress and thermal stress of $Ce_{0.8}Sm_{0.2}O_{2-\delta}$ based SOFC single cell.

$SmO_{1.5}$, just like $GdO_{1.5}$, then the relationship $\delta = 0.098\varepsilon$ is obtained for 973 K, and the relationship $\delta = 0.28\varepsilon$ is obtained for 1073 K. However, since there are no values in the literature for the amount of oxygen nonstoichiometry at 873 K, it was not possible to obtain a relationship between the amount of oxygen nonstoichiometry and the amount of chemically induced expansion. Due to the above, it is clear that oxygen nonstoichiometry is the cause of chemically induced expansion of $Ce_{0.8}Sm_{0.2}O_{2-\delta}$ electrolyte.

3.2. Stress analysis of the single cell taking into account chemically induced expansion

The authors conducted fracture evaluation testing of the single cell under a simulated operating condition [9], and observed the single cell in detail after testing. As a result, fracture patterns were classified into three types, as shown in Fig. 5: vertical cracking in the cathode, vertical cracking in the electrolyte, and delamination near the cathode/electrolyte boundary. From waveform analysis and frequency analysis obtained using the acoustic emission (AE) method, the authors successfully traced the fracture process of the single cell. As noted in Fig. 5, damage occurs from the surface of the cathode and near the boundary of the cathode/electrolyte around 640 K, and vertical cracking occurs in the electrolyte near 660 K. On the other hand, no damage at all was evident on the anode side. This may be because there is tensile stress on the cathode side, and compressive stress on the anode side. The likely cause of this stress is chemically induced expansion in the reducing environment of $Ce_{0.8}Sm_{0.2}O_{2-\delta}$ contained in the electrolyte and anode. First, let us discuss the fracture process described above based on the results of stress analysis. Fig. 6 shows calculation results for circumferential stress $\sigma_{\theta\theta}$, relating only to residual stress and thermal stress, without taking into account the effects of chemically induced expansion. Note that stress in the thickness direction and shear stress exhibited extremely small values compared to circumferential stress. Since stress was almost constant in all regions in the radial direction, only stress at the center part is shown. For the single cell used in this research, it is evident that there is almost no residual stress inside the electrolyte. Stress occurring inside the cathode and anode was a maximum of about 3 MPa, and this is in the range of about 3% or less of the fracture stress of the electrode material determined through SP testing. In terms of thermal stress, there was tensile stress of about 1 MPa on the electrolyte, and thus fracturing of the single cell is unlikely to occur due only to residual stress and thermal stress. In fact, no damage occurred in uniform heating experiments on the single cell using an atmospheric furnace, and this supports the above calculation results. Next, let us describe the results of stress analysis of the single cell under a simulated working environment, while taking into account chemically induced expansion. Fig. 7 shows the results of stress analysis of the center part of the single cell. Based on the data in Fig. 2, it shows the fracture strength of the electrolyte material and cathode material measured at 973 K. Since there are no 973 K results for the electrolyte material, values were obtained by interpolating the data. The respective fracture strengths of the electrolyte material and cathode material were approximately 160 MPa and 140 MPa. In this calculation, which took into account the chemically induced expansion of $Ce_{0.8}Sm_{0.2}O_{2-\delta}$, it is evident that compressive stress occurs on the anode side and tensile stress occurs on the cathode side. If the results in Fig. 6, which do not take into account chemically induced expansion, are compared with the results in Fig. 7, which do take into account chemically induced expansion, it is evident that the primary factor underlying cracking on the cathode side and cracking of the electrolyte is chemically induced expansion of the anode and the anode side of the electrolyte. Although tensile stress in the cathode and electrolyte is smaller than SP strength at 873 K, it is evident that the stress occurring at 973 K exceeds the SP strength. At 1073 K, there has only been a description of part of the stress inside the electrolyte, but this is because the stress occurring there exceeds the upper limit of the scale. It was found that

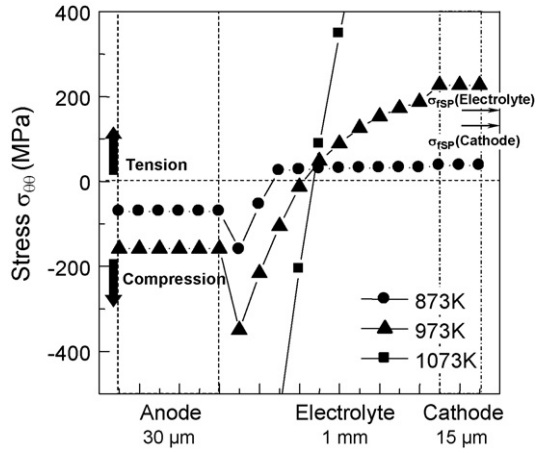

Fig. 7. Internal stress of $Ce_{0.8}Sm_{0.2}O_{2-\delta}$ based SOFC single cell under simulated operating conditions.

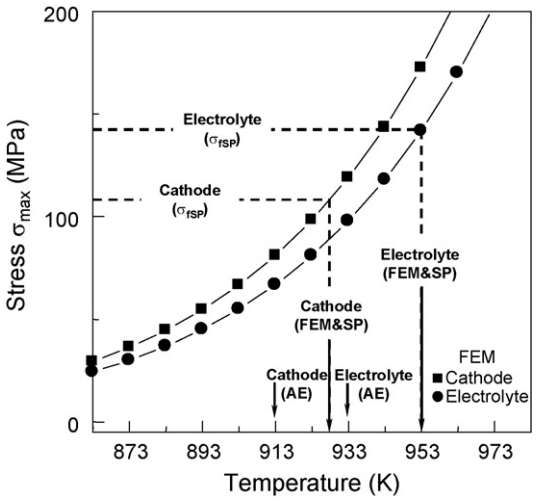

Fig. 8. Prediction of damage using FEM and observation of damage using AE method.

the SOFC single cell used in this research fractured primarily due to chemically induced expansion. In order to examine in detail the fracture conditions of the single cell's component materials, Fig. 8 shows the maximum circumferential stress which occurs inside the electrolyte and cathode in the temperature range of 873–973 K. In the diagram, arrows are used to indicate the temperature conditions at the time of vertical cracking of the cathode and electrolyte, estimated based on AE data. For the cathode, temperature is 640 K, and for the electrolyte it is 660 K. The fracture onset temperature, estimated based on stress analysis, is shown simultaneously for the cathode and electrolyte. The temperature at the time the maximum circumferential stress calculated using the finite element method exceeds the SP strength of the component material is taken to be the condition where fracture occurs. For the cathode this is 655 K, and for the electrolyte it is 680 K. The estimation results based on these stress analyses are comparatively close to the evaluation results based on AE data, and the difference is 5% for the cathode and 3% for the electrolyte. The SP strength used to estimate the fracture condition described above is the fracture strength under biaxial stress tension conditions. On the other hand, even in the stress state in the simulated working environment, the region at the center of the cell is almost in a biaxial tensile stress state, and it is likely to be close to the stress state in the SP test method. This supports the validity of using SP strength to estimate the fracture condition of the single cell in this research. Thus it has been shown to be possible to quantitatively estimate the condition where fracture occurs in the SOFC cell by using the strength of materials technique based on fracture strength described in this paper.

In the temperature range of chemically induced expansion illustrated in Fig. 3, it was found that chemically induced expansion cannot be ignored, and is clearly the primary cause of the induced stress. Under temperature conditions of 873 K or less, the amount of chemically induced expansion is expected to be extremely small, and in the temperature range over 873 K, designs will have to carefully take into consideration the factor of chemically induced expansion. In experiments on the single cell analyzed here, temperature conditions and environmental conditions of the anode and cathode were simulated, but the experiments were done in the open-circuit state with no flow of current. According to the results of recent preliminary stress analysis by the authors, the induced stress corresponding to the oxygen potential distribution during power generation is expected to be smaller than that in the open-circuit state described in this research. Consequently, it is likely that the stress analysis of the open-circuit state in this research can provide safety-related evaluation results for evaluating cell reliability.

Table 2
Oxygen ion, electron and hall conductivities of $Ce_{0.8}Sm_{0.2}O_{2-\delta}$.

Temperature	a_0 (S cm^{-1})[14]	σ_n^o (S cm^{-1})[15]	a_p^o (S cm^{-1}) [15]
873 K	0.0165	2.69×10^{-8}	3.12×10^{-5}
973 K	0.0347	4.37×10^{-7}	1.18×10^{-4}
1073 K	0.072	5.87×10^{-6}	4.22×10^{-4}
1173 K	0.129	4.98×10^{-5}	1.15×10^{-3}
1273 K	0.222	3.02×10^{-4}	2.81×10^{-3}

4. Conclusion

In this research, the component materials of a nonstoichiometric oxide based electrolytic SOFC were evaluated to determine their mechanical and chemical properties, and stress analysis was conducted on a single cell taking into account chemically induced expansion. This was done with the aim of establishing methods of SOFC evaluation and design. The cell used ($Ce_{0.8}Sm_{0.2}O_{2-\delta}$) as the electrolyte material, Ni–$Ce_{0.8}Sm_{0.2}O_{2-\delta}$ as the anode material, and $La_{0.6}Sr_{0.4}Co_{0.2}Fe_{0.8}O_{3-\delta}$ as the cathode material. The following summarizes the main conclusions of this research.

1. The high-temperature mechanical properties of the electrolyte, cathode and anode materials were evaluated using the SP testing method. For the cathode and anode materials, the elastic modulus decreased somewhat with rising temperature, but fracture strength tended to increase. For the electrolyte material, on the other hand, it was found that both the elastic modulus and fracture strength showed varying behavior which exhibited a minimum value. The mechanism underlying this is unknown, but the possibility that structural phase transition has an effect has been suggested, and in the future it will be necessary to examine not only temperature, but also the effects of factors such as oxygen partial pressure.
2. It was found that the amount of chemically induced expansion measured for $Ce_{0.8}Sm_{0.2}O_{2-\delta}$ exhibits a good linear relationship with the amount of oxygen nonstoichiometry, and that the chemically induced expansion of the material was induced by oxygen vacancy and change valence.
3. Fracture conditions were examined by stress analysis, using the finite element method and taking into account the chemically induced expansion of $Ce_{0.8}Sm_{0.2}O_{2-\delta}$. Based on this stress analysis, it was found that residual stress at fabrication of the single cell and thermal stress under high-temperature working conditions were small, but stress due to chemically induced expansion of $Ce_{0.8}Sm_{0.2}O_{2-\delta}$ exceeded the fracture stress of the component materials. This showed that stress due to chemically induced expansion was the main cause of the fracturing observed in this research, and that estimation of fracture conditions based on SP strength is an effective approach.

Acknowledgments

This work was made as a part of the research project on development of systems and elemental technology on SOFC, which was supported by the New Energy and Industrial Technology Development Organization (NEDO), Japan and the Global COE Program Grants of "International COE of Flow Dynamics", and Grant-in-Aid for Scientific Research (B) (No. 18360053) from the MEXT.

Appendix A.

The anode and the cathode are partly short-circuited by the electron flux through the electrolyte itself. In the open-circuit condition, the oxide ion flux ($J_{O^{2-}}$) and the electron flux (J_e) are balanced

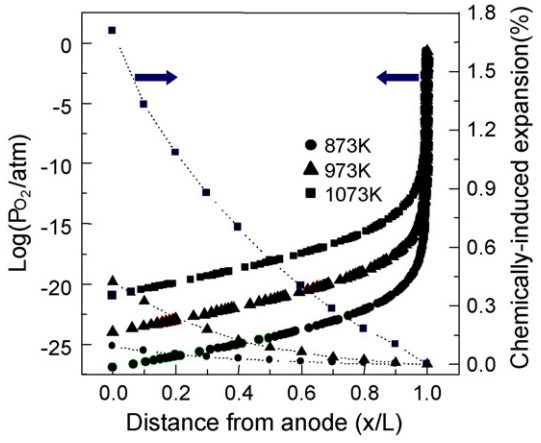

Fig. 9. Distribution of oxygen potential and lattice expansion induced in a plate of $Ce_{0.8}Sm_{0.2}O_{2-\delta}$.

every where inside the oxide [13]

$$J_{O^{2-}} + J_e = \frac{\sigma_{O^{2-}}}{2F}\frac{d\eta_{O^{2-}}}{dx} + \frac{\sigma_e}{F}\frac{d\eta_e}{dx} = 0 \quad (1)$$

Thus, the ratio of the electrochemical potential gradients of the oxide ion and the electron are determined by the ratio of the conductivities

$$J_{O^{2-}}x = \frac{RT}{4F}\int_{P_{O_2}(0)}^{P_{O_2}(x)} \frac{\sigma_{O^{2-}}\sigma_e}{\sigma_{O^{2-}} + \sigma_e} d\ln p_{O_2} \quad (2)$$

where R is the gas constant, T the temperature, F is the Faraday constant. The electronic current is carried by hole (p-type conduction) in the oxidizing atmosphere, and by electron (n-type conduction) in the reducing atmosphere,

$$\sigma_e = \sigma_n^0 {P_{O_2}}^{-1/4} + \sigma_p^0 {P_{O_2}}^{1/4} \quad (3)$$

Using Eq. (3),

$$J_{O^{2-}}x = \frac{RT}{4F}\int_{P_{O_2}(0)}^{P_{O_2}(x)} \left(\frac{\sigma_{O^{2-}}(\sigma_n^0 {P_{O_2}}^{-1/4} + \sigma_p^0 {P_{O_2}}^{1/4})}{\sigma_{O^{2-}} + \sigma_n^0 {P_{O_2}}^{-1/4} + \sigma_p^0 {P_{O_2}}^{1/4}}\right) d\ln p_{O_2} \quad (4)$$

Oxygen potential in the electrolyte $P_{O_2}(x)$ is defined as

$$\frac{x}{L} = \frac{\int_{P_{O_2}(0)}^{P_{O_2}(x)} \left(\frac{\sigma_{O^{2-}}(\sigma_n^0 {P_{O_2}}^{-1/4} + \sigma_p^0 {P_{O_2}}^{1/4})}{\sigma_{O^{2-}} + \sigma_n^0 {P_{O_2}}^{-1/4} + \sigma_p^0 {P_{O_2}}^{1/4}}\right) d\ln p_{O_2}}{\int_{P_{O_2}(0)}^{P_{O_2}(L)} \left(\frac{\sigma_{O^{2-}}(\sigma_n^0 {P_{O_2}}^{-1/4} + \sigma_p^0 {P_{O_2}}^{1/4})}{\sigma_{O^{2-}} + \sigma_n^0 {P_{O_2}}^{-1/4} + \sigma_p^0 {P_{O_2}}^{1/4}}\right) d\ln p_{O_2}} \quad (5)$$

The oxygen partial pressures and chemically induced expansions in the electrolyte were thus measure range of 873–1073 K. The calculated chemically induced expansion is summarized in Fig. 9 (Table 2).

References

[1] S.C. Singhal, Solid State Ionics 152 (2002) 405–410.
[2] M.C. Williamsa, et al., Journal of Power Sources 131 (1-2) (2004) 79–85, 14.
[3] Y. Watanabe, et al., Journal of Power Sources 61 (1-2) (1996) 53–59.
[4] A. Atkinson, Solid State Ionics 95 (1997) 249–258.
[5] H. Yakabe, et al., Journal of the Electrochemical Society 147 (11) (2000) 4071–4077.
[6] R. Krishnamurthy, B.W. Sheldon, Acta Materialia 52–7 (2004) 1807–1822.
[7] K. Sato, et al., Journal of Materials Science 39 (18) (2004) 5765–5770.
[8] K. Sato, et al., Solid State Ionics 180 (20–22) (2009) 1220–1225.
[9] K. Sato, et al., Journal of Testing and Evaluation 34 (3) (2006) 246–250.
[10] S. Sameshima, et al., Materials Chemistry and Physics 61 (1999) 31–35.
[11] A. Atkinson, T.M.G.M. Ramos, Solid State Ionics 129 (2000) 259–269.
[12] T. Kobayashi, et al., Solid State Ionics 126 (1999) 349–357.
[13] T. Kawada, H. Yokokawa, Key Engineering Materials, 125–126, Trans Tech Publications, Switzerland, 1997, pp. 187–248.
[14] H. Yahiro, et al., Solid State Ionics 36 (1989) 71–75.
[15] Y. Xiong, et al., Journal of The Electrochemical Society 151 (2004) A407–A412.